Scientific Research Publishing

Journal of Transportation Technologies, 2024, 14, 119-135
https://www.scirp.org/journal/jtts
ISSN Online: 2160-0481
ISSN Print: 2160-0473

Analytical Determination of Size and Location of Roadside Horizontal Sightline Offsets for Compound Curves

Timur Mauga

Department of Civil Engineering, The American University in Dubai, Dubai, UAE
Email: tmauga@aud.edu

How to cite this paper: Mauga, T. (2024) Analytical Determination of Size and Location of Roadside Horizontal Sightline Offsets for Compound Curves. *Journal of Transportation Technologies*, **14**, 119-135.
https://doi.org/10.4236/jtts.2024.141008

Received: December 21, 2023
Accepted: January 28, 2024
Published: January 31, 2024

Abstract

AASHTO's guideline for geometric design of highways and similar guidelines require that roadside areas on the inside of horizontal curves be cleared of high objects to provide stopping sight distance. The guidelines have analytical models for determining the extent of clearance, known as the horizontal sightline offset or clearance offset, for simple curves. Researchers in the past have developed analytical models for clearance offsets for spiraled and reverse curves. Very few researchers developed analytical models for available sight distances for compound curves. Still missing are models for horizontal sightline offsets and locations of the offsets for compound curves. The objective of this paper is to present development of analytical models and charts for determining horizontal sightline offsets and their locations for compound curves. The paper considers curves whose component arcs are individually shorter than stopping sight distance. The resulting models and the charts have been verified with accurate values determined using graphical methods. The models and the charts will find application in geometric design of highway compound curves.

Keywords

Sight Distance, Roadside Clearance Offsets, Compound Curves

1. Introduction

Guidelines for geometric design have analytical models for determination of clearance offsets on the inside of simple or circular horizontal curves. For example, the model for the offsets in the guideline by the American Association of State Highways and Transportation Officials (AASHTO) [1], is presented as Eq-

uation (1). This model is present in many geometric design guidelines. The model is the initial rational effort of providing design sight distance at curves of new projects. If designs do not camply by providing the clearance offset, the designs will not be approved by jurisdictions, and there is no justification for avoiding meeting the requirement.

$$M = R\left[1-\cos\left(\frac{28.65\times S}{R}\right)\right] \tag{1}$$

where

M is the clearance offset at the middle of a simple curve,

R is the radius of driver's path in the sharpest lane,

S is the design sight distance, here considered as stopping sight distance.

The model in Equation (1) was derived with an assumption that both a driver and a dangerous object are on curved part of a simple horizontal curve, as stated in the guideline. Therefore, the equation is best suited for curves that are longer than design sight distance. However, there is sufficient literature that has addressed clearance offsets for short and also for long simple curves [2]-[12], spiral curves [2] [13] [14], and reverse curves [15] [16] [17]. Many of these studies have been documented well in the newly developed design guideline for horizontal sightline offsets [18]. The only curve whose offsets have not been extensively studied analytically is the compound curve. Even the new design guideline for horizontal sightline offsets [18] explicitly states that its methods do not cover compound curves. In addition, the guideline [18] uses offsets already provided by other methods as its input.

Literature search for studies on horizontal offsets for compound curves found only a few studies, the earliest being that pioneered by Easa [19]. Easa developed models for available sight distances as functions of parameters of compound curves, given lateral clearance (or offset) to discrete roadside objects, and locations of drivers. In modeling, curve geometry and the offsets were inputs, and the outputs were available sight distances that vary with driver location. Easa [19] also developed interpolable design tables for minimum available sight distances and offsets to roadside objects stationed at specific points: point of curvature, middle of sharper arc, point of common curvature, middle of flatter arc, and point of tangency. However, the tables cannot be applied to determine maximum offsets analogous to Equation (1) except for curve geometry whose maximum offsets are at points of common curvature. It is obvious that maximum offsets cannot be at points of curvature or points of tangency for a given stopping sight distance. In addition, the maximum offsets cannot be at the middle of either sharper of flatter arcs since simple curves are the ones whose maximum offsets occur at their middles.

Hassan *et al.* [20] developed analytical models for determining available sight distances given geometry of types of horizontal alignments, including compound curves. The models were for sites with continuous roadside obstructions like retaining walls, fences, barriers, or back slopes. Inputs were curve geometry and

offsets to the roadside continuous obstructions. Although the paper did not present analytical equations for offsets at compound curves, probably due to limited space, it presented a sample design table that was generated with a software that was developed using analytical models. The sample table presents minimum available sight distance as a function of one offset (4.75 m), radii of arcs between 400 m and 2000 m, and central angles of compound arcs between 2˚ and 8˚. If the table presented data on the relationship between locations of tangency of sightlines and minimum available sight distance, and also for many offsets, it would also work for determination of maximum offsets and their locations.

Two papers, one by Liu and Wang [21] and the other by Liu [22], their titles state in the direction of having developed models for compound curves. Reviewing the papers revealed that what the authors called 3D compound curves were actually a combination of vertical curves and circular curves in overlap. The authors explicitly described that the projection of the 3D curves on the horizontal plane are simple circular curves. In addition, the papers [21] [22] do not state technical reasons that were based to choose the offsets which were used as inputs to models of available sight distances, and so did not Easa [19] and Hassan *et al.* [20].

The author of this paper is aware that the AASHTO's guideline recommends use of graphical methods in determining offsets for any type of horizontal curve when there is a technical reason for not applying Equation (1). The graphical method produces accurate offsets for all and compound curves. However, the method is tedious and time consuming. Tedium and time consumption are due to lack of mathematical representation of the method. Lack of mathematical representation makes it even mismatch universities' learning outcomes that require development of abilities to apply mathematics in formulating and solving complex engineering problems.

The objective of this paper is to present development of analytical models that will act as a rational way of determining clearance offsets for new compound curves as required by codes prior to approval of designs. The models use design sight distances and curve geometry to yield maximum offsets and locations of the offsets. The resulting offsets may therefore be applied as criteria of controlling location of roadside retaining walls, pillars, billboards, and back slopes so as to provide sight distances that are longer than design sight distances. The paper also presents graphical charts for determination of offsets and their locations, their verification, and comparison with values produced from other verified models. The methodology presented in this paper may further be used to extend the guideline for horizontal offsets (18) to cover compound curves.

2. Modeling

Engineering intuition may suggest that there are two maximum offsets at a compound curve, one for each circular arc. The intuition is accurate only for

compound curves whose each arc is at least long as design sight distance. In that case, Equation (1) is the appropriate model for its offsets and their locations. If one or both arcs are shorter than design sight distance, which is the focus of this paper, preliminary investigation suggests that there is only one maximum offset at a compound curve. That offset may be located within the sharper arc, at the point of common curvature, or within the flatter arc. Before modeling of the magnitude and location of the maximum offset, consider Figure 1 below for definition of terms.

Figure 1 presents a not-to-scale sketch of a compound curve. For the sake of simplification of modeling, Figure 1 represents a convention utilized in this paper. The convention is that a driver approaches from left to the right. The driver hence encounters the sharper arc first before the flatter arc. The dashed line in the figure is a sightline from an object "o" on the right to the driver "d" on the left. This setting or convention does not affect the magnitude of the offset where a driver encounters a flatter arc before its sharper arc. It affects the location of the offset relative to the beginning of the compound curve. Later near the end of this paper, it is presented how a design chart prepared with the convention is also applicable to curves where drivers encounter flatter arcs first before sharper arcs.

Using Figure 1, the following definitions apply:

R_1 is the radius of the flatter arc,

L_1 is the length of the flatter arc,

R_2 is the radius of the sharper arc,

L_2 is the length of the sharper arc,

PC is the point of curvature,

PCC is the point of common or compound curvature,

PT is the point of tangency,

PC-S is the origin and the start of influence area of a compound curve,

d is the location of a driver downstream of PC-S,

o is the location of a dangerous object, at distance S downstream of the driver,

α is the angle at which the sightline inclines from the approach tangent.

The methodology in this paper introduces new parameters which simplify complex modeling of many variables to linear equations. The parameters are simply thresholds of L_1 and L_2 which are used for determining model regimes based on location of objects "o" and offsets. The parameters are defined as:

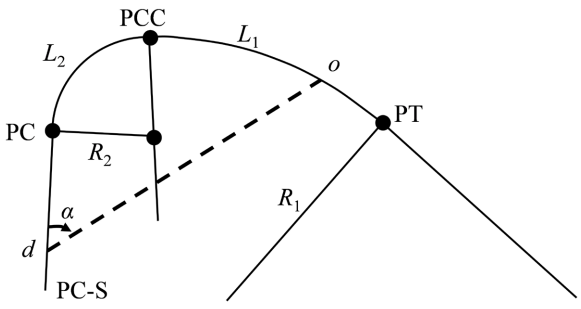

Figure 1. Geometric components of a compound curve.

1) L_{2cr} is the critical value of L_2 at which the maximum offset M is at PCC, for a given value of L_1. If L_2 is longer than L_{2cr}, the offset M is within L_2, if L_2 equals L_{2cr} the offset M is at PCC, and if L_2 is shorter than L_{2cr} the offset M is within L_1.

2) L_{2u} is the upper value of L_2 at which M is determined with the dangerous object "o" being on the driver's path at PT, for a given value of L_1. Values of L_2 that are smaller than L_{2u} correspond to the object being on the departure tangent, else, the object is within L_1.

3) L_{1cr} is the critical value of L_1 at which $L_{2cr} = L_{2u}$. The offset M is at PCC and the object is at PT.

The new parameters or thresholds of L_1 and L_2 were obtained after conducting geometric examination or inspection of a combination of S, L_1, L_2, R_1 and R_2. For a simple curve, location of M is simply fixed at the middle of the curve but for compound curves the location of M changes with how values of S, L_1, L_2, R_1 and R_2 combine, as stated in the definitions above. Ranges of values of L_1 and L_2 control modeling of M and its location. The ranges of values of L_1 and L_2 were observed to naturally form four (4) regimes or cases. Of the 4 cases, 2 are based on ranges of length L_1 relative to its critical value L_{1cr}. Each of the 2 cases of L_1 has 2 subcases based on ranges of lengths L_2 relative to L_{2cr} and L_{2u} values. The cases are:

Case A: Short L_1 (*i.e.* $L_1 \le L_{1cr}$). This case also has the property of $L_{2cr} \le L_{2u}$.

a - 1) $L_{2cr} \le L_2 \le L_{2u}$, the object is on the departure tangent.

b - 2) $L_{2u} < L_2 \le S$, the object is within the flatter arc L_1.

Case B: Long L_1 (*i.e.* $L_1 > L_{1cr}$). This case also has the property of $L_{2cr} > L_{2u}$.

a - 1) $L_{2cr} \le L_2 \le S$, the object is within L_1.

b - 2) $L_{2u} \le L_2 < L_{2cr}$, the object is within L_1.

2.1. Case A(a) $L_1 \le L_{1cr}$ and $L_{2cr} \le L_2 \le L_{2u}$

This case considers short arcs such that both a driver and an object are located on tangents. The conditions $L_1 < S$, $L_2 < S$ and $L_1 + L_2 \le S$ hold. The first step in modeling this case is determination of values of the parameters L_{2cr} and L_{2u}. Consider **Figure 2** for formulation of models for the parameters.

The critical length of the sharper arc L_{2cr} is obtained when the sightline is parallel to the common tangent at PCC (in **Figure 2**). This parallelism is due to the fact that maximum offsets must be simultaneously perpendicular to sightlines and driver paths. The value of α corresponding to M is thus the same as the central angle of the sharper arc, here denoted as Δ_2 as shown in **Figure 2**.

Determination of L_{2cr} is accomplished through programing by finding a positive value of L_2 that minimizes M for given values of L_1, R_1, R_2, and S, while maintaining the condition of the sightline being parallel to the common tangent at PCC. The objective function is presented by Equation (2a). The offset M in Equation (2a) is a sum of two parts as seen in **Figure 2** below. The first part is the first term in the right hand side of Equation (2a), as a component of x_2 in M. The second term is a component of the tangent length T_2 of the sharper arc L_2. Equation (3) presents the constraint.

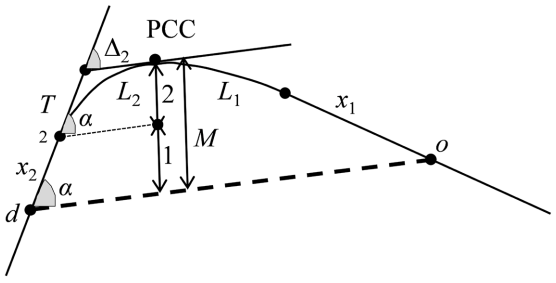

Figure 2. Geometric variables in Case A(a).

$$\min M = x_2 \cdot \sin(\alpha) + T_2 \cdot \sin(\alpha) \tag{2a}$$

Since $\alpha = \Delta_2$ and $T_2 = R_2 \cdot \tan(\Delta_2/2)$, α can be replaced with L_2/R_2 in the equation. Therefore:

$$\min M = x_2 \cdot \sin\left(\frac{L_2}{R_2}\right) + R_2 \cdot \tan\left(\frac{L_2}{2R_2}\right) \cdot \sin\left(\frac{L_2}{R_2}\right) \tag{2b}$$

Subject to:

$$x_2 + L_2 + L_1 + x_1 = S \tag{3}$$

where;

x_1 is the distance between PT and object location,

x_2 is the distance between PC and driver location.

The solution to Equation (2) is obtained at $L_2 = L_{2cr}$. The driver location d and the angle of inclination α corresponding to L_{2cr} are also at their critical values d_{cr} and α_{cr}, respectively. The Critical driver location d_{cr} and critical angle α_{cr} are calculated using the obtained critical length L_{2cr} as shown in Equation (4) and Equation (5).

$$\alpha_{cr} = L_{2cr}/R_2 = \Delta_2 \tag{4}$$

$$d_{cr} = S - x_2 = L_{2cr} + L_1 + x_1 \tag{5}$$

Figure 3 and Figure 4 present charts as an alternative way of obtaining L_{2cr} and d_{cr} without having to repetitively going through the programing procedure of solving Equation (2). These figures were developed after observing that compound curves with the same R_1/R_2 and L_1/S ratios have the same L_{2cr}/S and d_{cr}/S ratios. The (Figure 3 and Figure 4 below) are for limits of R_1/R_2 ratios of 1.5, 1.75, and 2 that are mentioned in the AASHTO's guide (1). The figures also include lines for R_1/R_2 ratios of 1.10 and 1.25 as additions. It is assumed that there are no compound curves with radii ratios that are smaller than 1.10.

The dashed line (in Figure 3) is the relationship between L_{1cr} and L_{2cr} while in Figure 4 the dashed line relates between L_{1cr} and d_{cr}. The dashed lines therefore separate areas for Case A and Case B in the figures.

To determine L_{2u} for a given L_1, the term x_1 is removed from Equation (3) and the dangerous object "o" is fixed at PT. It is worth to state that when solving for L_{2u}, the sightline is not conditioned to be parallel to the common tangent at PCC. However, when values of L_{2u} and L_{2cr} are equal, the sightline is parallel to the common tangent and the value of L_1 is also at its critical value L_{1cr}.

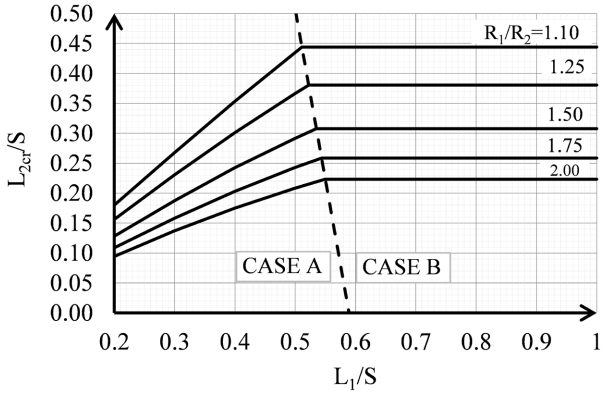

Figure 3. Relationships between L_1 and L_{2cr}.

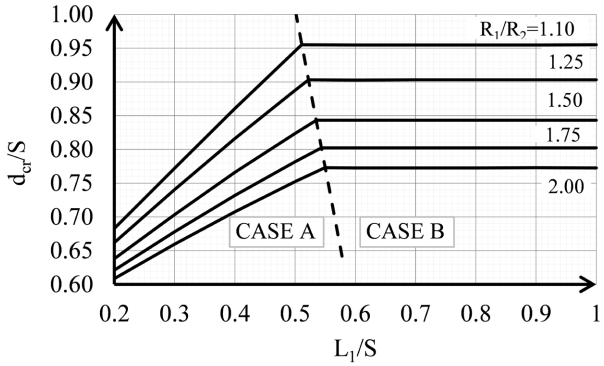

Figure 4. Relationships between L_1 and d_{cr}.

After obtaining the value of L_{2u}, the driver location corresponding to L_{2u} is calculated using Equation (6).

$$d_u = S - x_2 = L_{2u} + L_1 \tag{6}$$

The angle of inclination of a sightline corresponding L_{2u} is presented by Equation (7).

$$\alpha_u = \tan^{-1}\left(\frac{y_{PT}}{x_{PT} - d_u}\right) \tag{7}$$

where;

x_{PT} is the x-coordinate of PT measured along the approach tangent from PC-S,

y_{PT} is the y-coordinate of PT, positive on the inside of curve.

Figure 5 and Figure 6 present graphs that can be used to quickly determine values of L_{2u}, and d_u as functions of length of the flatter arc L_1.

Figure 7 presents a graph that can be used to determine values α_u. The parameter α_s is the angle of inclination of a sightline when $L_2 = S$ and hence $d = S$, with the object being at PCC.

After the parameters L_{2cr}, L_{2u}, and L_{1cr} are determined, equations for driver location and angle of inclination of a sightline corresponding to M are formed. It was found in this study that the equations are linear functions of lengths L_2 (of

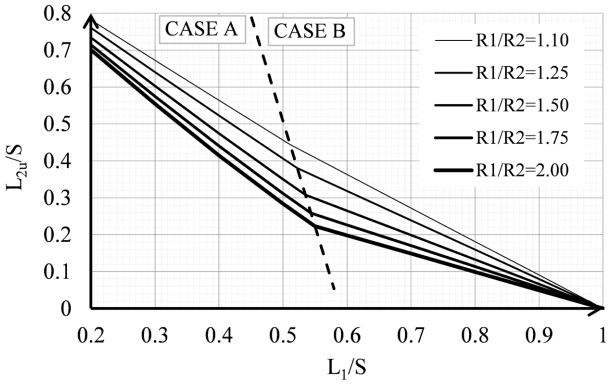

Figure 5. Relationships between L_1 and L_{2u}.

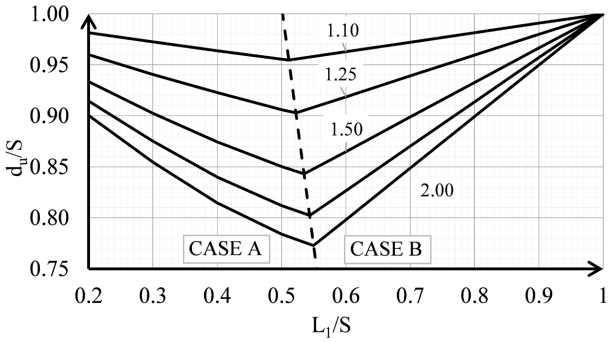

Figure 6. Relationships between L_1 and d_u.

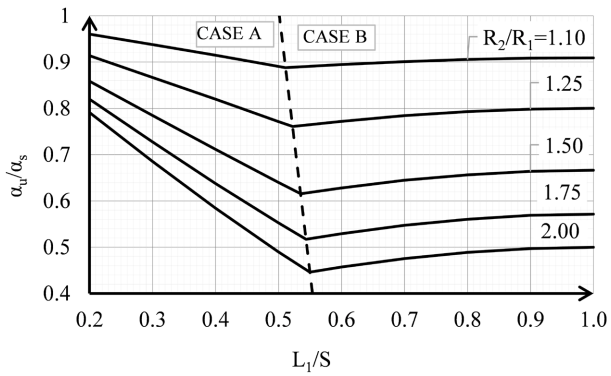

Figure 7. Relationships between L_1 and α_u.

sharper arcs). The linear equations are presented by Equation (8) and Equation (9). It can be seen that the fractions are slopes formed by using the range $L_{2cr} \le L_2 \le L_{2u}$ of L_2 for case A(a).

$$d_M = d_{cr} + \frac{d_u - d_{cr}}{L_{2u} - L_{2cr}}\left(L_2 - L_{2cr}\right),\ \ L_{2cr} \le L_2 < L_{2u} \tag{8}$$

$$\alpha_M = \alpha_{cr} + \frac{\alpha_u - \alpha_{cr}}{L_{1u} - L_{1cr}}\left(L_2 - L_{2cr}\right),\ \ L_{2cr} \le L_2 < L_{2u} \tag{9}$$

where;

d_M is the driver location corresponding to M,

α_M is the sightline angle corresponding to M.

These quantities d_M and α_M in Equation (8) and Equation (9), respectively, are then plugged in Equation (10) for the maximum offset. The value of the offset changes to that of Equation (1) if $L_2 = S$ at which d_M becomes S and the object is at PCC.

$$M = (S - d_M)\sin(\alpha_M) + R_2\left(1 - \cos(\alpha_M)\right) \tag{10}$$

Location of offset downstream of PC is given by Equation (11):

$$X_M = R_2\alpha_M \tag{11}$$

where;

X_M is the location of M downstream of PC.

The location of M may also be expressed as a linear function of L_2 as follows:

$$X_M = X_{cr} + \frac{X_u - X_{cr}}{L_{2u} - L_{2cr}}(L_2 - L_{2cr}),\ L_{2cr} \le L_2 \le L_{2u} \tag{12}$$

where:

$$X_{cr} = R_2\alpha_{cr} = R_2\Delta_{2cr} = L_{2cr},$$

$$X_u = R_2\alpha_u.$$

Note that values of L_2 that are shorter than L_{2cr} in Case A are not considered in the modeling since they are shorter than minimum values recommended in the AASHTO's guideline [1].

2.2. Case A(b) $L_1 \le L_{1cr}$ and $L_{2u} < L_2 \le S$

This case considers short flat arcs and long sharp arcs. Since all values of L_2 are longer than L_{2u}, dangerous objects are on the short flat arcs. Values of L_{2u}, d_u, and α_u are determined as described in Case A(a) above. Equations for driver location and inclination of sightline corresponding to M are as presented by Equation (13) and Equation (14).

$$d_M = d_u + \frac{S - d_u}{S - L_{2u}}(L_2 - L_{2u}),\ L_{2u} \le L_2 < S \tag{13}$$

$$\alpha_M = \alpha_u + \frac{\alpha_S - \alpha_u}{S - L_{2u}}(L_2 - L_{2u}),\ L_{2u} \le L_2 \le S \tag{14}$$

where:

$$\alpha_S = 0.5S/R_2\ .$$

These d_M and α_M values are inputs to Equation (10) above for calculating the offset M. The location of the offset is calculated using Equation (15).

$$X_M = X_u + \frac{0.5S - X_u}{S - L_{2u}}(L_2 - L_{2u}),\ L_{2u} \le L_2 \le S \tag{15}$$

2.3. Case B(a) $L_1 > L_{1cr}$ and $L_{2cr} < L_2 \le S$

This case considers that both flat and sharp arcs are long. Equations for critical driver locations and critical sightline angles are the same as Equations (4) and

(5) in Case A(a) except that L_1 is long and x_1 is not applicable. The critical values of driver location and angle of sightline inclination are calculated with Equation (16) and Equation (17).

$$\alpha_M = \alpha_{cr} + \frac{\alpha_S - \alpha_{cr}}{S - L_{2cr}}\left(L_2 - L_{2cr}\right),\ L_{2cr} \le L_2 \le S \tag{16}$$

$$d_M = d_{cr} + \frac{S - d_{cr}}{S - L_{2cr}}\left(L_2 - L_{2cr}\right),\ L_{2cr} \le L_2 \le S \tag{17}$$

The maximum offset is calculated with Equation (10) presented above in Case A(a). The location of the offset is given by Equation (18):

$$X_M = X_{cr} + \frac{0.5S - X_{cr}}{S - L_{2cr}}\left(L_2 - L_{2cr}\right),\ L_{2cr} \le L_2 \le S \tag{18}$$

2.4. Case B(b): $L_1 > L_{1cr}$ and $L_{2u} < L_2 < L_{2cr}$

This is the case that involves long flat arcs and short sharper arcs. Equations for critical driver locations and critical sightline angles are the same as Equations (4) and (5) in Case A(a). Equations for driver locations and sightline angles corresponding to the maximum offset M are as follows:

$$\alpha_M = \alpha_u + \frac{\alpha_{cr} - \alpha_u}{L_{2cr} - L_{2u}}\left(L_2 - L_{2u}\right),\ L_{2u} \le L_2 \le L_{2cr} \tag{19}$$

$$d_M = d_u + \frac{d_{cr} - d_u}{L_{2cr} - L_{2u}}\left(L_2 - L_{2u}\right),\ L_{2u} \le L_2 \le L_{2cr} \tag{20}$$

Location of the offset M is downstream of PCC. The offset is calculated with Equation (21). The three components of the equation are presented in the not-to-scale Figure 8.

$$M = \left(S - d_M\right)\sin\left(\alpha_M\right) + \left(R_2 - Q\right)\cos\left(\theta\right) + R_1\left[1 - \cos\left(\theta\right)\right] \tag{21}$$

The term θ is the central angle intercepting the arc between PCC and X_M. The central angle is given by Equation (22) and illustrated by Figure 8.

$$\theta = \frac{X_M - L_2}{R_1} = \alpha_M - \Delta_2 \tag{22}$$

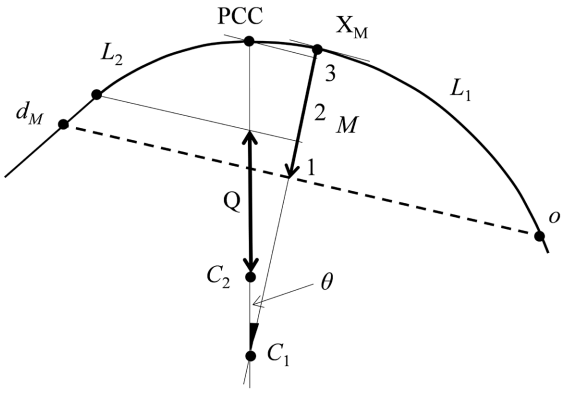

Figure 8. M with three components, located within L_1.

Length Q in the second term of Equation (21) is given by Equation (23) and shown in Figure 8.

$$Q = \frac{R_2}{\sin\left(0.5\pi + \alpha_M - \Delta_2\right)} \sin\left(0.5\pi - \alpha_M\right) \tag{23}$$

Location of the offset is within the flatter arc [unlike in Cases A and B(a)]. That location is determined with the linear Equation (24):

$$X_M = X_u + \frac{X_{cr} - X_u}{L_{2cr} - L_{2u}}\left(L_2 - L_{2u}\right),\ L_{2u} \le L_2 \le L_{2cr} \tag{24}$$

where

$$X_u = L_{2u} + \left(\alpha_u - \Delta_{2u}\right)R_1,$$

$$\Delta_{2u} = L_{2u}/R_2.$$

Note that in this sub case, values of L_2 that are shorter than L_{2u} are not considered in the modeling since they are shorter than minimum values recommended in the AASHTO's guideline [1].

3. Calculation Example

Consider a highway with speed of 40mi/h and stopping sight distance of 305 ft. The maximum offset M for a compound curve with R_1 = 750 ft, L_1 = 180 ft, R_2 = 500 ft, and L_2 = 150 ft is found by first classifying the compound curve whether it is Case A or B.

$$\frac{R_1}{R_2} = \frac{750}{500} = 1.5$$

$\frac{L_1}{S} = \frac{180}{305} = 0.59 > 0.535$ this is Case B in Figure 3.

$\frac{L_1}{S} = 0.59$ gives a value of $\frac{L_{2cr}}{S} = 0.31$ on the vertical axis of Figure 3.

Therefore, $L_{2cr} = 0.31 \times 305 = 94.55$ ft.

$\frac{L_1}{S} = 0.59$ gives a value of $\frac{L_{2u}}{S} = 0.275$ on the vertical axis of Figure 5.

$$L_{2u} = 0.275 \times 305 = 83.88 \text{ ft.}$$

Since $L_{2u} < L_{2cr} < L_2$, it is Case B(a).

The critical value of sightline angle is calculated with Equation (4).

$$\alpha_{cr} = L_{2cr}/R_2 = 94.55/500 = 0.1891 \text{ rads.}$$

The critical value of driver location is read on Figure 4 as $d_{cr}/S = 0.84$.

The critical driver location is $d_{cr} = 0.84 \times 305 = 256.2$ ft.

Equations (16) and (17) are then used to calculate driver location and sightline angle corresponding to M as presented in Equation (25) and Equation (26).

$$\alpha_M = 0.1891 + \frac{0.5 \times 305/500 - 0.1891}{305 - 94.55}\left(150 - 94.55\right) = 0.22 \text{ rads} \tag{25}$$

$$d_M = 256.2 + \frac{305 - 256.2}{305 - 94.45}\left(150 - 94.55\right) = 269.06 \text{ ft.} \tag{26}$$

Resulting values in Equation (25) and (26) are plugged in Equation (10) as follows:

$$M = (305 - 269.06)\sin(0.22) + 500(1 - \cos(0.22)) = 19.91 \text{ ft.} \quad (27)$$

The offset location downstream of PC is calculated with Equation (18), as Equation (28) below.

$$X_M = 94.55 + \frac{0.5 \times 305 - 94.55}{305 - 94.55}(150 - 94.55) = 109.82 \text{ ft.} \quad (28)$$

This location is not mid-arc of L_2 as it would have been for a simple curve with R_2 = 500 ft and L_2 = 150 ft.

4. Design Charts and Discussion

Figure 9 presents a design chart for compound curves with R_1/R_2 = 1.5. The input on the horizontal axis is a ratio of length of a sharper arc to S while the output is the offset ration M/M_{AASHTO} on the vertical axis. M_{AASHTO} is the offset that results from applying Equation (1) at a situation where the sharper arc is long as S. The first result to note is that for a given length of a sharper arc (*i.e.* L_2/S ratio), an offset for compound curve increases with increase in length of its flatter arc as long as $L_1 < S$. The chart also shows that for a given length of a flatter arc, the maximum offset generally increases with increase in the length of the sharper arc as long as $L_2 < S$.

In Figure 9, the dashed line is for offset ratios of sites whose flat arcs are long as critical values L_{1cr} (here presented by the ratio L_{1cr}/S = 0.535). At low values of L_2/S, lines below the dashed line are for Case A(a) while those above it are for Case B(b). Lines in Case A(b) and Case B(a) are spot-on with the dashed line. Lines in Case B(a) are spot-on with the dashed line starting at the critical value of L_{2cr}/S = 0.308 to 1. Lines in Case A(b) are spot-on with the dashed line starting at the their individual values of L_{2i}/S to 1. For the ranges in which lines in Case A(b)

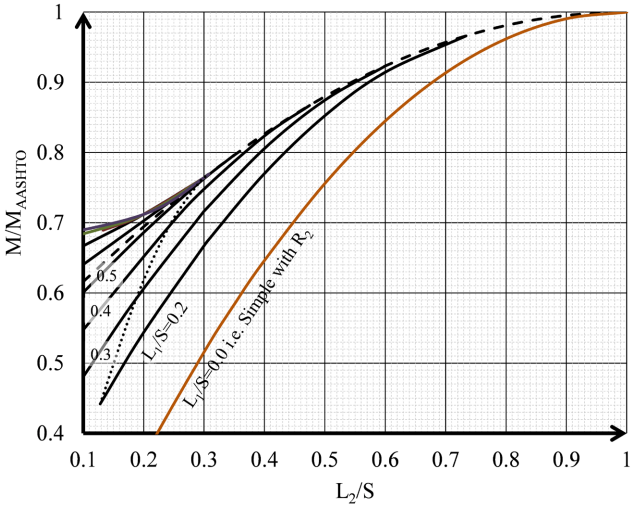

Figure 9. Offset factor M/M_{AASHTO} as a function of length of sharp arc factor L_2/S.

and Case B(a) are spot-on with the dashed line, the offset ratios are the same as those of the dashed line $L_{1cr}/S = 0.535$. The dotted line is for offsets where sharper arcs are at their critical lengths or critical L_2/S ratios *i.e.* L_{2cr}/S.

If the calculation example presented in the previous section was to use the chart to determine the offset, the procedure would have been brief as follows:

$$\frac{L_1}{S} = \frac{180}{305} = 0.59$$

$$\frac{L_2}{S} = \frac{150}{305} = 0.49$$

Drawing a vertical line at the value of 0.49 on the horizontal axis meets the curve for $L_1/S = 0.59$ (spot-on with the dashed line) to give an offset ratio of 0.875 on the vertical axis.

Equation (1) yields an offset of:

$$M = 500\left[1 - \cos\left(\frac{305}{2\times 500}\right)\right] = 23.08 \text{ ft} \tag{29}$$

The needed offset is $M = 0.875 \times 23.08 = 20.2$ ft which is comparable to 19.91 ft depending on the precision of reading the charts in both methods.

Figure 10 presents a chart for locations of the maximum offsets as ratios of S. The locations are measured from PC to downstream. The dashed line is for the critical value of L_1/S which is $L_{1cr}/S = 0.535$ for $R_1/R_2 = 1.5$. In the figure, all lines are above the line for simple sharp curves *i.e.* $L_1/S = 0$. Since maximum offsets are at middles of simple curves, for compound curves the offsets are downstream of the middle of the sharper arcs, except for $L_2/S = 1$.

In Figure 10, at low values of L_2/S, lines below the dashed line are for Case A(a) while those above it are for Case B(b). Lines in Case B(b) are spot-on with each other and they join the dashed line at the critical value of L_2/S which is $L_{2cr}/S = 0.308$. Lines in Case A(a) meet with the critical line $L_{1cr}/S = 0.535$ at their individual values of L_{2u}/S. Lines for Case A(b) and B(a) are spot-on with the critical dashed line hence their location ratios are read on the dashed line $L_{1cr}/S = 0.535$. The dotted line is for location ratios for compound curves with critical values of L_2/S. The location ratios corresponding to the dotted line are for the

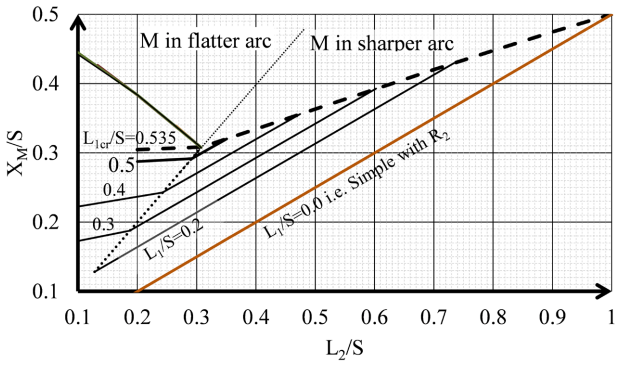

Figure 10. Location factor X_M/S (from PC) as a function of length of sharp arc L_2/S.

PCC station. Location values of lines on the right of the dotted line imply that maximum offsets M are in sharper arcs while those on the left of the dotted line imply that the offsets are in flatter arcs.

For the example presented in the previous section, values of L_2/S and L_1/S are 0.49 and 0.59, respectively. The values result in an X_M/S ratio of 0.36. The location of the offset is thus:

$$X_M = 0.36 \times 305 = 109.8 \text{ ft}.$$

The value 109.8 ft is the same as 109.82 ft obtained earlier using equations. The maximum offset is located 109.8 ft downstream of PC or 220.2 ft upstream of PT. If configuration of a compound curve begins with a flatter arc, the location of M will still be measured from PC but with a small modification to its math. Suppose that geometry of the above example begins with the flatter arc. The location of M is determined as follows:

$$X_M = L_1 + L_2 - \left(X_M/S \text{ ratio}\right) \times S$$

$$X_M = 180 + 150 - 0.36 \times 305 = 220.2 \text{ ft} \quad \text{from PC of flat arc.}$$

Note, since quantities in **Figure 9** and **Figure 10** are unitless, the charts may be applied in imperial and metric systems.

5. Verification of the Charts

This section presents a few examples of maximum offsets and their locations that are verified with offsets that are generated using the graphical procedure. Although the procedure is not an advanced method, offset values generated with it are accurate and are trusted by researchers and practitioners. For example, the AASHTO guideline [1] recommends its use for cases that don't have analytical models for offsets. Also, Hassan *et al.* [20] verified their models with the graphical method. **Table 1** below presents the verification data. Scenarios 1 and 2 include data from past studies by Easa [19] and Hassan *et al.* [20], respectively, for the sake of comparison. The first scenario uses data from **Table 1** by Easa [19] whose geometry is available sight distance of S_{av} = 158 m, $\Delta_1 = \Delta_2 = 10^\circ$, sharper R_2 = 200 m, and an offset of 10m at station PCC. The second scenario uses data from table 5 by Hassan *et al.* [20] as available sight distance of S_{av} = 143 m, $\Delta_1 = \Delta_2 = 6^\circ$, sharper R_2 = 400 m, and an offset of 4.75 m. The lengths are converted to feet.

The data in **Table 1** show that offsets and their locations, determined with the proposed charts (**Figure 9** and **Figure 10**) match well with those determined with the graphical procedure. The small differences between graphical values and values from the charts are due to variation of precision in reading the charts, expected in practice. A reader is advised to conduct the graphical procedure to verify the values. The offset values determined with the design table developed by Easa [19] is a little greater than those determined with both the chart and the graphical method. The offset value determined with table 5 by Hassan *et al.* [20] is the same as that determined with the analytical method in this paper and the graphical procedure.

Table 1. Comparison of models' offset with graphical offsets.

Scenario:		1	2	3	4	5	6
Speed (mi/h)				50	40	35	30
S (ft)		518.37	469.16	425	305	250	200
L_1 (ft)		171.70	206.04	340	305	200	120
L_2 (ft)		114.47	137.36	170	244	200	160
R_2 (ft)		656.17	1312.34	700	500	350	250
Offset M (ft)	Figure 9	32.64	15.59	26.50	22.64	21.64	19.34
	Graphical	32.62	15.57	26.40	22.64	21.66	19.36
	Easa (19)	32.81	-	-	-	-	-
	Hassan *et al.* (20)	-	15.58	-	-	-	-
Location from PC (ft)	Figure 10	110.42	130.27	141.95	136.64	112.00	89.60
	Graphical	110.44	130.30	141.41	136.84	112.01	89.46
	Easa (19)	114.47	-	-	-	-	-

6. Conclusions

This paper presents development of analytical models for determination of clearance offsets on the inside of compound curves. The paper introduces three geometric parameters which simplify the problem to a set of linear equations. The paper demonstrates how to apply the equations but also presents design charts. In addition, the paper presents verification of the models and the charts with accurate offsets prepared using the graphical method. The charts use unitless quantities hence they can be used in imperial and metric systems.

In research, the equations and the charts form a foundation on which to base future research on determination of minimum offsets at other than locations of maximum offsets, and also extension to 3D alignments.

In practice, geometric designers are required to provide clearance offsets that ensure provision of design sight distance at curves. Failure to comply with the requirement ends in disapproval of designs by jurisdictions. The equations and charts presented in this paper provide an analytical and rational way of determining the offsets required by design guidelines without having to incur negatives of graphical methods but yield as accurate offsets. The equations and charts will be suited for sites with alignments that are level, are on constant grade, or have flat vertical curvature, or have no vertical curvature. Inclusion of vertical curvature is in the next phase based on what has been developed in this paper.

Conflicts of Interest

The author declares no conflicts of interest regarding the publication of this paper.

References

[1] The American Association of State Highways and Transportation Officials (AASHTO) (2018) A Policy on Geometric Design of Highways and Streets. The American Association of State Highways and Transportation Officials, Washington DC.

[2] Raymond, W.L. (1972) Offsets to Sight Obstructions near the Ends of Horizontal Curves. *ASCE Journal of Civil Engineering*, **42**, 71-72.

[3] Glennon, J.C. (1978) Effects of Sight Distance on Highway Safety. Transportation Research Board (TRB) State of the Art Report No. 6, Washington DC, 64-77.

[4] Olson, P.L., Cleveland, D.E., Fancher, P.S. and Schneider, L.W. (1984) Parameters Affecting Stopping Sight Distance. Research Report NCHRP 270, Washington DC.

[5] Cleveland, D.E., Kostyniuk, L.P., Waissi, G.R., Olson, P.L. and Fancher, P.S. (1985) Stopping Sight Distance Parameters. Transportation Research Record No. 1026, Washington DC, 13-23.

[6] Waissi, G.R. and Cleveland, D.E. (1987) Sight Distance Relationships Involving Horizontal Curves. Transportation Research Record No. 1122, Washington DC, 96-107.

[7] Easa, S.M. (1991) Lateral Clearance to Vision Obstacles on Horizontal Curves. Transportation Research Record No. 1303, Washington DC, 22-32.

[8] Lovell, D.J. (1999) Automated Calculation of Sight Distance from Horizontal Geometry. *Journal of Transportation Engineering*, **125**, 297-304. https://doi.org/10.1061/(ASCE)0733-947X(1999)125:4(297)

[9] Lovell, D.J., Jong, J.C. and Chang, P.C. (2001) Improvement to Sight Distance Algorithm. *Journal of Transportation Engineering*, **125**, 283-288. https://doi.org/10.1061/(ASCE)0733-947X(2001)127:4(283)

[10] Ameri, M., Rostami, T., Mansourian, A. and Salehabadi, E. (2012) New Method for Determination of Driver Sight Distance from Roadside Obstacles on Horizontal Curves. *Journal of Basic and Applied Scientific Research*, **2**, 141-158.

[11] Mauga, T. (2014) Horizontal Clearance Offsets to Objects Higher than Sightlines. *Transportation Research Record*, **2436**, 23-31. https://doi.org/10.3141/2436-03

[12] You, Q.C. and Easa, S.M. (2016) Innovative Roadside Design Curve of Lateral Clearance: Roadway Simple Horizontal Curves. *Journal of Transportation Engineering*, **142**, 1-10. https://doi.org/10.1061/(ASCE)TE.1943-5436.0000889

[13] Mauga, T., Ghanma, M. and Ahmed, K. (2013) Roadside Clearance Limit on Horizontal Curves with Transition Arcs: Sites with Circular Arcs Shorter than Sight Distance. *Transportation Research Record*, **2358**, 20-28. https://doi.org/10.3141/2358-03

[14] You, Q.C. and Easa, S.M. (2017) Innovative Roadside Design Curve of Lateral Clearance: Roadway Spiraled Horizontal Curves. *Journal of Transportation Engineering*, **143**, 1-11. https://doi.org/10.1061/JTEPBS.0000046

[15] Easa, S.M. (1994) Design Considerations for Highway Reverse Curves. *Transportation Research Record*, **1445**, 1-11.

[16] Mauga, T. (2015) Minimum Roadside Clearance Offsets on the Inside of Reverse Curves Based on Flat Spirals. *Journal of Transportation Technologies*, **5**, 169-184. https://doi.org/10.4236/jtts.2015.53016

[17] You, Q.C. and Easa, S.M. (2020) Roadside-Curve Lateral Offsets for Roadway Reverse Horizontal Curves with Intermediate Tangents. *Canadian Journal of Civil En-*

gineering, **47**, 382-394. https://doi.org/10.1139/cjce-2018-0547

[18] Potts, I.B., Douglas, W.H., Daniel, J.C., Eric, T.D. and Bashir, H. (2019) Design Guidelines for Horizontal Sightline Offsets. NCHRP Research Report No. 910, Washington, DC. https://doi.org/10.17226/25537

[19] Easa, S.M. (1993) Lateral Clearance Needs on Compound Horizontal Curves. *Journal of Transportation Engineering*, **119**, 111-123. https://doi.org/10.1061/(ASCE)0733-947X(1993)119:1(111)

[20] Hassan, Y., Said M.E. and Abd El Halim, A.O. (1995) Sight Distance on Horizontal Alignments with Continuous Lateral Obstructions. *Transportation Research Record*, No. 1500, Washington DC, 31-42.

[21] Liu, C. and Wang, Z.R. (2012) Deriving Sight Distance on a Compound Sag and Circular Curve in a Three Dimensional Space. *International Journal of Science and Technology*, **1**, 297-303. https://doi.org/10.1260/2046-0430.1.3.297

[22] Liu, C. (2013) Exact Sight Distance Determination on Compound Vertical and Horizontal Curves in the Presence of Road Barriers. *International Journal of Science and Technology*, **2**, 159-166. https://doi.org/10.1260/2046-0430.2.2.159